

# Analysis of the discrete wavelet coefficients using a Watermark Algorithm

Sandra L. Gomez Coronel, Marco A. Acevedo Mosqueda, Ma. Elena Acevedo Mosqueda and Ricardo Carreño Aguilera.

**Abstract**—This paper analyses the performance of the Discrete Wavelet Transforms (DWT) in a watermark algorithm designed for digital images. This algorithm employs a perceptive mask and a normalization process. The watermark insertion is done through the spread-spectrum technique, which is still, after a couple of decades, one of the safest ways to disguise the presence of the watermark in the digital image to the human eye. The algorithm is evaluated by establishing which wavelet coefficient provides the best accommodation in the watermark, i.e., it is not noticeable and will resist the various attacks, both intended and unintended. Different objective metrics are used—Peak Signal to Noise Ratio (PSNR), Multi-Scale Structural Similarity Index (MSSIM) average, correlation coefficient- and Bit Error Rate (BER) to determine which coefficient performs better in the insertion and extraction of the watermark.

**Index Terms**—Discrete Wavelet Transform, Image normalization, Perceptive Mask, Spread Spectrum, Watermarking.

## I. INTRODUCTION

Nowadays most humans deal with information in a digital format (audio, video, or image). Although its immediate access represents an advantage, we cannot forget that the contents are also vulnerable to any kind of manipulation. By shielding digital data, we can safely share information, even through unsafe channels, preventing illegal reproductions or unauthorized alterations to original material. One way to achieve this is through watermarks, which purpose is to protect copyright in digital contents by inserting information into the digital file -that is to be authenticated. The watermark should remain imperceptible, robust, and hard to remove or alter; however, it must remain detectable when verifying the data. Over the last two decades, various watermarking techniques have been developed around three features: robustness, safety, and legibility. In the practice, the first two qualities work as opposites, because when imperceptibility is the focus, there is a tendency to loose robustness. When one intends to prevent visual alterations to the image, some of its perceptible areas remain unmodified, making the watermark vulnerable to both intentional and unintentional attacks. In addition, the legibility aspect seeks for the watermark to be detected, and/or extracted, at wish without any setbacks.

The different techniques found in the state-of-the-art demand the ability to insert the watermark in two levels: the

spatial and the transform domains. The goal is to achieve an imperceptible watermark, impervious to all attacks because of its robustness. As a rule, the techniques suited for the spatial domain lack robustness, because the pixels (or pixel clusters) that must be marked are directly modified. To avoid perceptible changes, one option is to alter the least significant bit (LSB), or a cluster of them [1], [2], [3], [4], nevertheless, by modifying the intensity levels of the pixels, we end up with techniques that hold a small amount of robustness. This is the reason why it is preferable to work on the transform domain (Discrete Wavelet Transform (DWT), Discrete Cosine Transform (DCT), Discrete Fourier Transform (DFT), Contourlet Transform, or Hermit transform (HT)), thus making more difficult to eliminate or modify the watermark [5], [6], [7], [8], [9], [10], [11], [12], [13], [14]. There are also some techniques that take into account the features of the Human Vision System model (HVS) to hide the watermark [15], [16], [17], [18], [19]. These techniques are on the increase because of the positive results they produce in regards to intended and unintended attacks. Four approaches stand out: [16], [17], [20], [21]. The first one shows satisfactory results in JPEG compression and cropping, while successfully disguising the watermark through the DWT sub detail bands texture and luminance. [17] takes [16] as a frame of reference, but uses the Contourlet transform. Finally, in order to support more geometric attacks, algorithms like [20], [21] have resorted to normalized method of the marked image, preventing in this manner variations to affine transformations. Also there are other algorithms that proposed use Zernike moments or Scale-Invariant Feature Transform (SIFT) [22], [23], [24] to improve the selection places to insert the watermarking, ensuring robustness against attacks and quality image. Zernike moments have ability to provide faithful image representation and they are insensitivity to noise, whereas SIFT can extract feature points robust against various attacks, such as rotation, scaling, JPEG compression, and also transformation.

In light of the previous results, in this paper we suggest the evaluation of a watermark algorithm that uses a normalized process, as well as a perceptive watermark, so to guarantee robustness and prevent it to be perceptible. After dispersing the mark in the DWT domain, the watermark must be inserted in the spatial domain. The evaluation consists in establishing which is the best coefficient to disperse the watermark while obtaining the best results in relation to the robustness and quality in the marked image. Two aspects have then to be considered: on the one hand, even when the significant perceptual coefficients of the high-frequency subbands preserve

Sandra L. Gomez Coronel, Departamento de Ingeniería, Instituto Politécnico Nacional, UPIITA. Av. IPN No. 2580. Col. La Laguna Ticomán, Postcode 07340. Ciudad de México. México e-mail: ( sgomezc@ipn.mx).

Marco. A. Acevedo-M, Ma. Elena Acevedo-M and Ricardo Carreño A. are with Instituto Politécnico Nacional, Sección de Estudios de Posgrado e Investigación, ESIME Zacatenco, Ciudad de México.

Manuscript received X; revised X.

the invisibility of a watermark, these will remain vulnerable to common processing attacks; on the other, the low-frequency subbands coefficients cannot be modified, because such a change would be perceptible. Therefore, we suggest dispersing the watermark in the mid-frequency subbands coefficient (mid-low, and mid-high). We proposed to extract the watermarking not just its detection, because we use as watermarking legible information. Some algorithms use logos or pseudo random sequences, so the information amount is great. In this particular paper we use watermarks lengths between 60 and 104 bits. In order to allow the reader to comprehend the process, this paper presents the following structure: section two summarizes the DWT theory, while the third explains the proposal regarding the mark algorithm and watermark extraction; section four holds the results of each coefficient tests-to that end, several metrics were applied: Peak Signal-to-Noise Ratio (*PSNR*), correlation coefficient, Multi-Scale Structural Similarity Index (*MSSIM*) average, and Bit Error Rate (*BER*). The last section encloses the conclusions.

**A. Discrete Wavelet Transform (DWT)**

The wavelet transform can be understood as the decomposition of a group of basic functions, which can be obtained through scales and samplings of a mother wavelet. The analysis of this transform results in a group of wavelet coefficients that shows how close to a particular base function the signal actually is. Therefore, it is to be expected for any general signal to be represented as a decomposition of wavelets. This means that each original wave form can be synthesized through the constant addition of essential blocks that have different sizes and amplitude. Although there are many wavelet types, the Discrete Wavelet Transform (DWT) is the most common when processing images. The actual goal of the DWT is to convert a continuous signal into a discrete one through a sampling process. The latter is based on a multiresolution analysis, i.e. a specific number of decomposition levels in the wavelets domain. These are retrieved through a variety of digital filters (low-pass and high-pass filters).

1) *Two-Dimensional Wavelet Transform*: Digital images are two-dimensional digital signals, represented by a *I* matrix of *m**x**n* dimensions. The two-dimensional discrete wavelet transform requires [25]:

- 1) A scaling function  $\varphi(x, y)$
- 2) Three two-dimensional wavelets  $\psi^H(x, y)$ ,  $\psi^V(x, y)$ ,  $\psi^D(x, y)$

Each one is the product of the  $\varphi$  one-dimensional scaling function and the corresponding  $\psi$  wavelet, so that (Eq. 1) to (Eq. 4):

$$\varphi(x, y) = \varphi(x)\varphi(y) \tag{1}$$

Is a separable scaling function, and:

$$\psi^H(x, y) = \psi(x)\psi(y) \tag{2}$$

$$\psi^V(x, y) = \psi(x)\psi(y) \tag{3}$$

$$\psi^D(x, y) = \psi(x)\psi(y) \tag{4}$$

are separable wavelets.

These wavelets measure the intensity variations or gray levels.  $\psi^H$  measures the variations along the columns, that is, where the horizontal image’s details are preserved, and the mid-low frequencies (*h* coefficient) held.  $\psi^V$  measures the variations along the rows, where the vertical details and mid-high frequencies (*v* coefficient) are enclosed.  $\psi^D$  measures the diagonal details as well as the high frequencies (*d* coefficient). The *a* coefficient holds the low frequencies and contains a compressed version of the original signal. The insertion of a watermark must occur in areas in which human vision is less sensible to changes, i.e. in the detail coefficients [26], [27]. Figure 1 shows a scheme of the two-dimensional wavelet decomposition, for a  $x[n, m]$  signal.

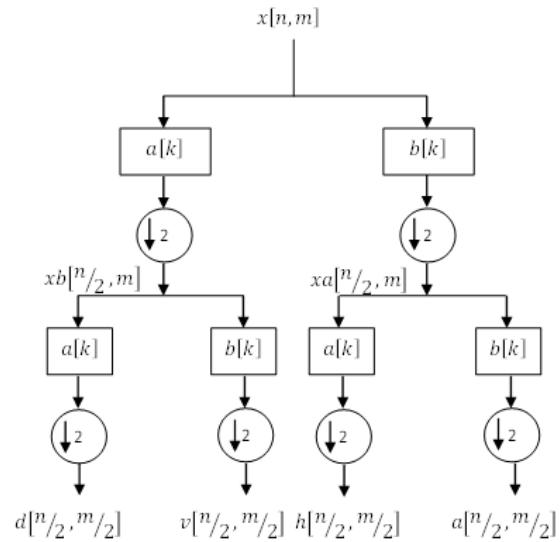


Fig. 1. Wavelet signal decomposition  $x[n, m]$

**II. WATERMARKING ALGORITHM**

The purpose of this paper is to evaluate which of the wavelet coefficients is more suitable to disperse the watermark, by ensuring the marked image robustness and visual quality. Some approaches [26], [27], [28] have been set out so to establish which is the wavelet that guarantees better results based on the aforementioned parameters. This particular work focuses on to evaluate which wavelet coefficient produces the best results by inserting a watermark. The suggested algorithm uses a normalized method [20] to avoid alterations in the marked image due to possible geometric transformations. It also utilizes a perceptive mask that allows for the watermark to remain hidden, in the chosen coefficient, to the human eye. Each process is explained in the next sections.

**A. Image normalization**

The normalized process is based on the invariant moments theory [29]. For a  $f(x, y)$  image with  $M \times N$  dimensions, these steps must be followed.

- 1) The  $f(x, y)$  image must be translated into  $f_1(x, y) = f(x_a, y_a)$ , with a center equivalent to the central mass of  $f(x, y)$ , and is given by (Eq. 5):

$$\begin{pmatrix} x_a \\ y_a \end{pmatrix} = A \begin{pmatrix} x \\ y \end{pmatrix} - d \quad (5)$$

where (Eq. 6) and (Eq. 7) are:

$$A = \begin{pmatrix} 1 & 0 \\ 0 & 1 \end{pmatrix} \quad (6)$$

$$d = \begin{pmatrix} d_x \\ d_y \end{pmatrix} \quad (7)$$

The values  $d_x, d_y$  are given by the geometric moments (Eq. 8):

$$d_x = \frac{m_{10}}{m_{00}}, d_y = \frac{m_{01}}{m_{00}} \quad (8)$$

where (Eq. 9):

$$m_{pq} = \left[ \sum_{x=0}^{M-1} \sum_{y=0}^{N-1} x^p y^q f(x, y) \right] \quad (9)$$

- 2) Next, a shearing transform is applied in X direction to the  $f_1(x, y)$  image, to get  $f_2(x, y)$  using (Eq. 10):

$$A = \begin{pmatrix} 1 & \beta \\ 0 & 1 \end{pmatrix} \quad (10)$$

where  $\beta$  is determined by (Eq. 11):

$$\mu_{30} + 3\beta^3 \mu_{12} + \beta^3 \mu_{30} \quad (11)$$

and  $\mu_{pq}$  are the image's central moments.

- 3) A shearing transform is applied in Y direction to the  $f_2(x, y)$  function, to get  $f_3(x, y)$  with the matrix (Eq. 12):

$$A = \begin{pmatrix} 1 & 0 \\ \gamma & 1 \end{pmatrix} \quad (12)$$

where (Eq. 13):

$$\gamma = \frac{\mu_{11}}{\mu_{20}} \quad (13)$$

where  $\mu_{pq}$  are the central moments of image resulting of step 2.

- 4) The  $f_3(x, y)$  image is scaled in both directions ( $x, y$ ) to get  $f_4(x, y)$ , with the matrix (Eq. 14):

$$A = \begin{pmatrix} \alpha & 0 \\ 0 & \delta \end{pmatrix} \quad (14)$$

where  $\alpha$  and  $\delta$  are determined by the size for the image obtained in the previous step.

The  $f_4(x, y)$  image is the normalized image of the original  $f(x, y)$  image, so that the watermark can be built as a function of the invariance, and becomes robust against different manipulations.

## B. Perceptive Mask

In order to achieve an imperceptible watermark in the image to which it is inserted, it must be hidden through a mask. We call masking to the phenomenon by which a signal's visibility diminishes in favor of another one that disguises the original image. The design of the perceptive mask uses the human visual system model (HVS). Some works [14], [16], [17] take into consideration the texture and the luminance contents of the image subbands. Here, however, the perceptive mask is designed according to the Schouten brightness model [30]. It establishes that the brightness representation is invariant to the properties of a luminous source, as well as to the observation conditions. Watson [31], on the contrary, suggested designing the mask through a quantization matrix that depended on the image, thus producing a minimal erroneous bits rate for a given perception error, and vice versa. Originally, the Discrete Cosine Transform (DCT) was used, but the algorithm here described employs the HT. This adjustment was suggested in [32]. The decision to work with the HT responds to its properties, as well as to the existing similarities between the functions of the synthesis filters, and those that model the receptive fields of the HSV. In [32], the contrast is calculated through the Hermite coefficients, and through the luminance masking. Eq. 15, Eq. 16 and Eq. 17 demonstrate the calculations pertaining to each one of the elements.

$$C = \left[ \sum_{i=1}^m \sum_{j=1}^{n-m} C_{i,j}^2 \right]^{\frac{1}{2}} \quad (15)$$

where  $C_{i,j}$  represents the Hermite Transform Cartesian Coefficients.

$$C_{thr} = k_0 \left( C_{min} + \left| \frac{B^\alpha - L_{min}^\alpha}{B^\alpha + L_{min}^\alpha} \right|^{\frac{1}{\alpha}} \right) \quad (16)$$

where:

$k_0$ , is a constant.

$C_{min}$ , is the minimal contrast present when a luminance level exists.

$L_{min}$ , represents the maximum contrast sensitivity [32].

$\alpha$ , is a constant that includes values in the  $[0, 1]$  interval.

$C_{thr}$ , is the contrast masking.

$B$ , is the brightness map proposed by [30].

and

$$M = k_1 \max(C_{thr}, C^\beta C_{thr}^{1-\beta}) \quad (17)$$

where:

$k_1$  is a constant.

$M$  is the perceptive mask.

## C. Watermark Insertion

The watermark insertion process is illustrated in figure 2, and includes the following steps:

- 1) Calculate the normalization parameters of the original image  $I(n \times m)$ , to obtain  $I_N(\hat{n} \times \hat{m})$ .

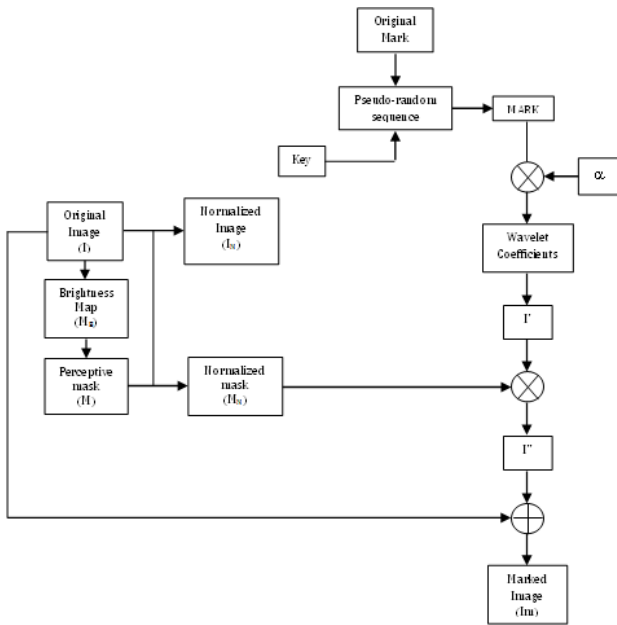


Fig. 2. Watermark insertion process based on the suggested  $x[n,m]$  algorithm

- 2) Create the binary watermark with a  $n\{0,1\}$  length, starting from a numeric or alphanumeric code.
- 3) Generate  $p_i$  pseudo-random sequences, using a private key  $k$ , where  $i = 1, \dots, l$  and  $l$  represents the number of message bits applied as the watermark. Each sequence has  $\{-1, 1\}$  values and  $\hat{n} \times \hat{m}$  dimensions.
- 4) Calculate the brightness map  $B$  of the original image  $I(n \times m)$  [30].
- 5) Calculate the perceptive mask  $M$  according to (Eq. 17)
- 6) To obtain  $M_N$ , normalize the perceptive mask  $M$  using the normalization parameters resulting after step 1.
- 7) Modulate the watermark with the  $p_i$  sequences to obtain  $W_a$  (Eq. 18)

$$W_a = \sum_{i=1}^l (2m_i - 1)p_i \quad (18)$$

where  $m_i$  is the  $i$ -th bit of the watermark.

- 8) Generate the null wavelet coefficients and choose those in which the watermark will be inserted.
- 9) Insert the watermark through (Eq. 19):

$$\tilde{I}_{k,l}(i, j) = \alpha W_a \quad (19)$$

where:

$\alpha$  is a strength control parameter.

$W_a$  is the modulated watermark.

$\tilde{I}_{k,l}$  is the modified wavelet coefficient.

- 10) Calculate the inverse wavelet transform of the coefficients to get  $\hat{I}$ .
- 11) Multiply  $\hat{I}$  with the normalization mask  $M_N$  and apply the inverse normalization process to get  $\hat{\hat{I}}$ .
- 12) The final watermark  $W$  is inserted in the original image in additive form through (Eq. 20):

$$I_m = I + \hat{\hat{I}} \quad (20)$$

#### D. Watermark Extraction

To extract the watermark a correlated detector is to be used during the process, so that, when comparing the resulting correlation value of the sample with the original, one must consider if it is a bit 1 or a bit 0.

### III. TEST RESULTS

We used 36 different images of dimensions  $512 \times 512$  as well as two watermarks with 64 bits and 104 bits in length, respectively. The goal was to determine which wavelet coefficient,  $h$  or  $v$ , was more suitable to insert the watermark. Likewise, the strength control parameter  $\alpha$  was modified (0.05 to 0.14 with increases of 0.1) in order to establish the value that throws the best results regarding the quality of the marked image, and the mark extraction. Since one of the purposes was to obtain a broad view, various types of metrics were used: Peak to Signal-to-Noise Ratio (*PSNR*), that measures the statistical variations present between the original and the watermarked image, the Multi-Scale Structural Similarity Index (*MSSIM*) average and the coefficient correlation. In addition, the Bit Error Rate (*BER*) allowed the calculation of the modified bits quantity existing in each inserted mark. The averages of every metric helped us to compare the coefficients. Figures 3 to 7 show coefficient averages for both watermark lengths.

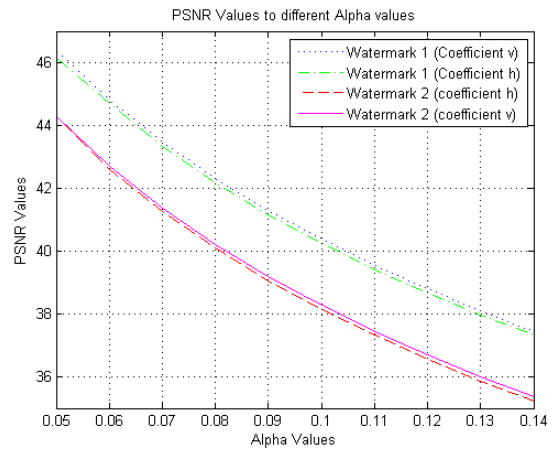


Fig. 3. *PSNR* average for each coefficient ( $h$  and  $v$ ), after the insertion of both watermarks.

Figures 6 and 7 illustrate the watermark extraction. To make the insertion in the  $v$  coefficient entails more modified bits during the extraction process, thus obtaining a bigger *BER* in that specific coefficient. For the 64 bits length watermark, the erroneous bits average maintains up to a 3 bits average during the extraction, whereas the  $h$  coefficient has a 2 bit average. Now, when dealing with 104 bits long watermark, we face a similar situation: the best extraction results are related to the coefficient  $h$ -the modified bits average is of 4 bits-, while in the coefficient  $v$  are near to 6 bits. We concluded that to achieve a lower error average during the extraction, coefficient  $h$  is better to insert the watermark. Figures 8 and 9 show both the original and the modified Lena image using the coefficient  $h$ .

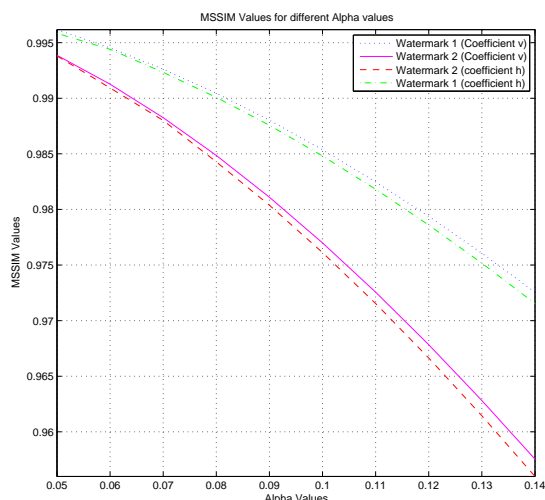


Fig. 4. *MSSIM* for each coefficient ( $h$  and  $v$ ), after the insertion of both watermarks.

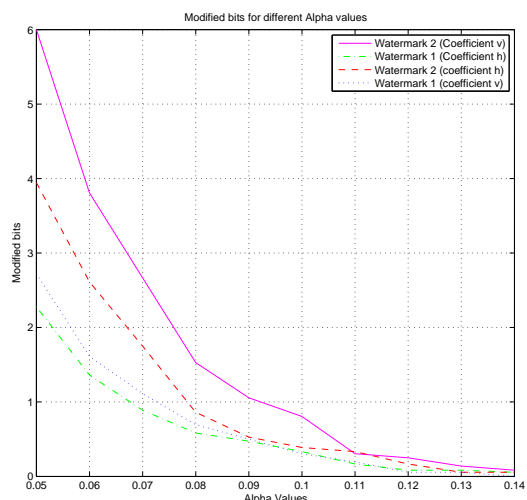


Fig. 6. Each coefficient ( $h$  and  $v$ ) average, after the insertion of both watermarks.

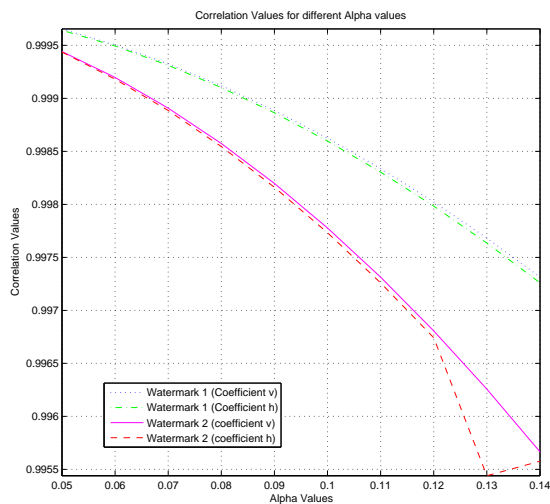


Fig. 5. Correlation coefficient average ( $h$  and  $v$ ), after the insertion of both watermarks.

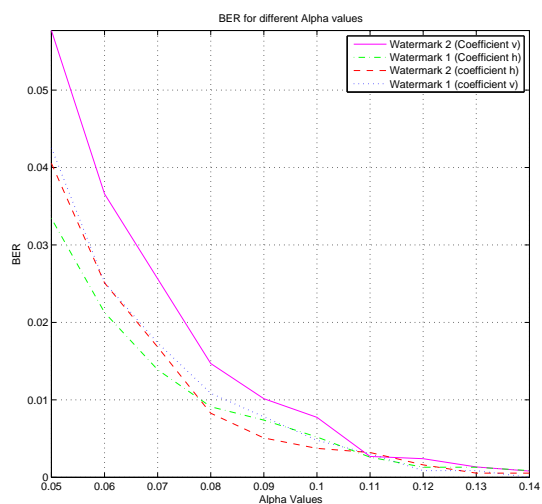


Fig. 7. BER average for each coefficient ( $h$  and  $v$ ), after the insertion of both watermarks

### A. Evaluation of the Algorithm Attacks

In order to determine if a similar result was obtained with attacks-after the watermark insertion in both  $h$  or  $v$  coefficients- three different types were tested: Gaussian filter, and Shearing in horizontal and vertical orientations. Concerning the Gaussian filter, a size  $N \times N$ , linear filtering was used; the filter average was 0 and the standard deviation was 0.5. Both parameters remained constant in all the tests. The only alteration was the  $N$  filter size-from 1 to 9, in 1 increments. Now, in case of shearing, in both cases  $X$ ,  $Y$ , deformation was applied from 0 to 1 in 0.04 increments, which resulted in 26 distortions in each instance. These attacks were applied to demonstrate the performance during common processing and geometric attacks. Table I illustrates a representative sample of the failed attacks on 7 different images (these are commonly

utilized in this type of tests). Each column indicates the total figure of failed attacks with an extraction of 2 modified bits at least. Despite of it, is it possible to recognize watermark.

As shown in table I it appears to be meaningless which coefficient is used to insert the watermark, since most attacks are unsuccessful. However, it is important to stress that the watermark extraction works better when the coefficient  $h$  is used. Therefore, we concluded that the latter is the best option when inserting a watermark, because it will accomplish both robustness and quality in the marked image. Finally, it is a fact that, for these sample images, we have a robust algorithm against to common processing and geometric attacks.

Figures 10, 11 and 12 show Lena image after all of the attacks that hold the highest parameters. Each one extracted perfectly the inserted watermark in the coefficient  $h$ .

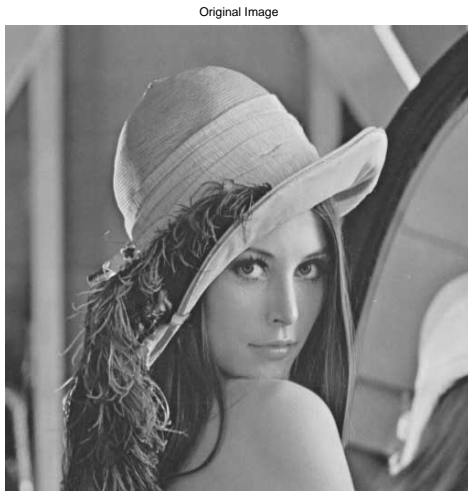


Fig. 8. Original image Lena



Fig. 9. Watermarked image Lena



Fig. 10. Lena image after horizontal shearing

TABLE I  
FAILED ATTACKS FOR EACH IMAGE TESTED.

Image	Coeff.	Watermark	G. Filter	Shearing X	Shearing Y
Lena	h	1	9	22	8
		2	9	26	14
	v	1	5	24	23
		2	8	24	21
Babbon	h	1	5	26	22
		2	5	26	23
	v	1	3	4	26
		2	5	3	25
Barbara	h	1	5	26	23
		2	5	26	23
	v	1	5	24	21
		2	5	22	26
Boat	h	1	9	25	21
		2	9	26	22
	v	1	9	22	8
		2	9	24	8
Peppers	h	1	5	24	18
		2	1	21	21
	v	1	5	8	10
		2	9	6	9
Pirate (actor)	h	1	9	3	20
		2	9	0	18
	v	1	5	26	17
		2	5	26	21
Bridge	h	1	5	26	26
		2	5	26	26
	v	1	5	10	24
		2	9	14	25



Fig. 11. Lena image after vertical shearing

Watermark Image with Gaussian Filter



Fig. 12. Lena image after Gaussian filter

#### IV. CONCLUSION

This paper presents the evaluation of a robust watermarking technique in order to determine the most suitable wavelet coefficient ( $h$  or  $v$ ) in which to insert a  $l$  length watermark. According to the tests, we can firmly conclude that the coefficient  $h$  shows the best performance in regards to the insertion and extraction of the mark, as well in relation to resisting attacks. The values of the *PSNR* averages are close to 40dB even when the insertion force is altered. Such values indicate that the human eye is incapable of registering any difference in the marked image [30], [31]. Now, the remaining metrics (*MSSIM* and correlation coefficient) show averages closer to the unit, which means that, even when an image suffers alterations, they will stay hidden when compared to the original. The marked Lena image (Figure 9) shows that, visually, there are no noticeable changes when compared to the original image. As noted, one of the parameters that must be taken into account in the algorithm design is the robustness, because it is usually exposed to both unintended and intended attacks [34], the latter have more relevance because they specifically seek to affect the watermark. With this in mind, the algorithm, through a representative sample, was evaluated through a geometric attack that distorts the horizontal and vertical planes, and a common processing attack applying Gaussian filter, the results show that the coefficient  $h$  allows a better extraction of the watermark. Table I helps us conclude that, even when it is possible to make an extraction with both coefficients, more extractions are likely to occur in the various attacks when using the coefficient  $h$ . If we also add the metrics employed to measure the quality of the marked image, the values remain close to the ideal. Hence, the  $h$  coefficient is where the watermark must be placed.

#### ACKNOWLEDGMENT

The authors would like to thank for financial support at Instituto Politécnico Nacional IPN (COFAA, EDI and SIP), CONACyt-SNI.

#### REFERENCES

- [1] S. Kimpan and A. Lasakul and S. Chitwong. Variable block size based adaptive watermarking in spatial domain. *IEEE International Symposium on Communications and Information Technology*, Vol. 1, pages 374–377. 2004.
- [2] G. Voyatzis and I. Pitas. Applications of toral automorphism in image watermarking *IEEE International Conference on Image Processing*, Vol. 2, pages 237–240. 1996.
- [3] Ch-Ch. Chang and J-Y. Hsiao, Ch-L. Chiang. An Image Copyright Protection Scheme Based on Torus Automorphism *Proceedings of the First International Symposium on Cyber Worlds*, pages 217–224. 2002.
- [4] I. J. Cox and J. Kilian, F. T. Leighton and T. Shamoon. Secure spread spectrum watermarking for multimedia *IEEE Transactions on Image Processing*, Vol. 6, No. 12, pages 1673–1687. 1996.
- [5] S.D. Lin and Ch-F. Chen. A robust DCT-based watermarking for copyright protection *IEEE Transactions on Consumer Electronics*, Vol. 46, No. 3, pages 415–421. 2000.
- [6] C. M. Kung and J. H. Jeng and T. K. Truong. Watermark technique using frequency domain *14th International Conference on Digital Signal Processing*, Vol. 2, pages 729–731. 2002.
- [7] H. Zhou and Ch. Qi and X. Gao. Low luminance smooth blocks based watermarking scheme in DCT domain *International Conference on communications, circuits and systems proceedings*, Vol. 1, pages 9–23. 2006.
- [8] R. Dugad and K. Ratakonda and N. Ahuja. A new wavelet-based scheme for watermarking images *International Conference on Image Processing*, Vol. 2, pages 419–423. 1998.
- [9] Z. Dawei, Ch. Guanrong and L. Wenbo. A chaos-based robust wavelet-domain watermarking algorithm *Chaos, Solitons, & Fractals*, Vol. 22, No. 1, pages 47–54. 2004.
- [10] H. Dehghan and S. Ebrahim Safav. Robust Image Watermarking in the Wavelet Domain for Copyright Protection *CoRR*, Vol. abs/1001.0282. 2010.
- [11] Ch-Ch. Chang and K-N. Chen and M-H. Hsieh. A robust public watermarking scheme based on DWT *Sixth International Conference on Intelligent Information Hiding and Multimedia Signal Processing*, pages 21–26. 2010
- [12] E. Candés and L. Demanet and D. Donoho and L. Ying. Fast discrete curvelet transforms *Multiscale Modeling & Simulation*, Vol. 5, No. 5, pages 861–899. 2005.
- [13] M. Jayalakshmi and S. N. Merchant and U. B. Desai. Blind Watermarking in Contourlet Domain with Improved Detection *International Conference on Intelligent Information Hiding and Multimedia Signal Processing*, pages 449–452. 2006.
- [14] N. Baaziz, B. Escalante-Ramírez and O. Romero. Image Watermarking in the Hermite Transform Domain with Resistance to Geometric Distortions *Proceedings of the SPIE Optical and Digital Image Processing*, pages 70000X1–70000X11. 2008.
- [15] R. B. Wolfgang, C. I. Podilchuck and E. J. Delp. Perceptual watermarks for digital images and video *Proceedings of the IEEE*, Vol. 87, No. 7, pages 1108–1126. 1999.
- [16] M. Barni, F. Bartolini and A. Piva. Improved wavelet-based watermarking through pixel-wise masking, *IEEE Transactions on Image Processing*, Vol. 10, No. 5, pages 783–791. 2001.
- [17] N. Baaziz. Adaptive watermarking schemes based on a redundant contourlet transform, *IEEE International Conference on Image Processing*, Vol. 1, pages 1221–4. 2005.
- [18] A. Saadane. Watermark strength determination based on a new contrast masking model *Proceedings of the SPIE-IS& T Electronic Imaging*, Vol.5020, pages 107–114. 2003.
- [19] S. Marano, F. Battisti, A. Vaccari, G. Boato and M. Carli. Perceptual data hiding exploiting between-coefficient contrast masking *Image Processing: Algorithms and Systems VI*, Vol. 618, pages 68121E1–68121E10. 2008.
- [20] P. Dong, J. G. Brankov, N. P. Galatsanos, Y. Yang and F. Davaone. Digital watermarking robust to geometric distortions *IEEE Transactions on Image Processing*, Vol. 14, pages 2140–2150. 2005.
- [21] M. Cedillo and M. Nakano and H. Pérez. Robust Watermarking to Geometric Distortion Based on Image Normalization and Texture Classification *51st Midwest Symposium on Circuits and Systems*, pages 245–2489. 2018.
- [22] X-Ch. Yuan and Ch.M. Pun. Feature extraction and local Zernike moments based geometric invariant watermarking *Multimedia Tools and Applications*, Vol. 72, No.1, pages 777–799. 2014.
- [23] C. Singh and S. K. Ranade. Image adaptive and high capacity watermarking system using accurate Zernike moments *IET Image Processing*, Vol. 8, No. 7, pages 373–382. 2014.

- [24] J. Xu. and L. Feng. A feature-based robust digital image watermarking scheme using image normalization and quantization *2nd International Symposium on Intelligence Information Processing and Trusted Computing (IPTC)*, pages 67–70. 2011.
- [25] I. Orea. Thesis: Marcas de agua robustas en imágenes digitales con formato *Escuela Superior de Ingeniería Mecánica y Eléctrica ESIME Zacatenco, IPN*. 2005.
- [26] E. Brannock and et al. Watermarking with Wavelets: Simplicity leads to robustness *Proceedings of IEEE Southeastcon*, pages 587–592. 2008.
- [27] S. Lee and et al. Reversible Image Watermarking Based on Integer-to-Integer Wavelet Transform *IEEE Transactions on Information Forensics and Security*, Vol. 2, No. 3, pages 321–330. 2007.
- [28] S. P. Mayit and M. K. Kundu. Performance improvement in spread spectrum image watermarking using Wavelets *International Journal of Wavelets, Multiresolution and Information Processing*, Vol. 9, pages 1–33. 2011.
- [29] M. K. Hu Visual Pattern Recognition by Moment Invariants *IRE Transactions on Information Theory*, Vol. 8, No. 2, pages 179–187. 1962.
- [30] G. Schouten Thesis: Luminance-Brightness Mapping: the Missing Decades *Technische Universiteit Eindhoven*. 1992.
- [31] A. B. Watson. DCT quantization matrices visually optimized for individual images *Proceedings of the SPIE Human Vision, Visual Processing, and Digital Display IV*. 1993.
- [32] B. Escalante, P. López, and J. L. Silvan SAR Image Classification with a Directional-Oriented Discrete Hermite Transform *Proceedings SPIE Image and Signal Processing for Remote Sensing VII*. 2002.
- [33] J. R. Ohm Bildsignalverarbeitung fuer Multimedia-Systeme <http://bs.hhi.de/user/ohm/download/bvm-kap1&2.pdf>
- [34] B. L. Gunjal and R. R. Manthalkar Discrete Wavelet Transform based Strongly Robust Watermarking Scheme for Information Hiding in Digital Images *Third International Conference on Emerging Trends in Engineering and Technology*, pages 124–129. 2010.

**Sandra L. Gomez Coronel** Received her BS degree in Communications and Electronics Engineering from Escuela Superior de Ingeniería Mecánica y Eléctrica at Instituto Politécnico Nacional (IPN) in 2003, her MSc degree in Telecommunications Engineering in 2008 from SEPI ESIME Zacatenco (IPN) and her PhD degree from Universidad Nacional Autónoma de México in 2014. Her research interests include digital signal processing, specifically image processing and their applications. Also she has several years as bachelor professor at UPIITA (IPN).

**Marco A. Acevedo Mosqueda** He was born in Mexico City in July 19th, 1968. He received his BS degree in Communications and Electronics Engineering in 1992 and his MSc degree with specialization in Electronics in 1996 from Escuela Superior de Ingeniería Mecánica y Eléctrica at Instituto Politécnico Nacional. Currently, he is a professor in ESIME. His main research area is Digital Signal Processing and Telecommunications.

**Ma. Elena Aevedo Mosqueda** Received her BS degree in Engineering with specialization in Computing from the Escuela Superior de Ingeniería Mecánica y Eléctrica (ESIME) at Instituto Politécnico Nacional (IPN) in 1996. She has been teaching at ESIME since 1994. She received her MSc degree with specialization in Computing from the Centro de Investigación y de Estudios Avanzados (CINVESTAV) in 2001. She received her PhD from the Centro de Investigación en Computación (CIC) at IPN in 2006. Her main research area is Artificial Intelligence and Associative Memories.

**Ricardo Carreño Aguilera** He studied a bachelor in Communications and Electronics Engineering with specialization in control at ESIME-ZACATENCO IPN, a master in business administration at the University of Querétaro and a PhD in systems engineering in the post-graduate and research area at ESIME-ZACATENCO IPN. Currently he is developing research in complex systems and artificial intelligence.